Optimal Actuator Layout Design on Circular Plate for High-Precision Smart Space Structure

ICAST2015: 26th International Conference on Adaptive Structures and Technologies
October 14-16th, 2015, Kobe, Japan

ICAST2015 #046

Optimal Actuator Layout Design on Circular Plate for High-Precision Smart Space Structure

Tomohiko Naka[1], Nozomu Kogiso[1*], Tadashige Ikeda[2], and Hiroaki Tanaka[3]

[1] Department of Aerospace Engineering, Osaka Prefecture University, Sakai, Japan.
[2] Department of Aerospace Engineering, Nagoya University, Nagoya, Japan.
[3] Department of Aerospace Engineering, National Defense Academy of Japan, Yokosuka, Japan.

Abstract

Space antennas for space exploration misssions using high frequency wave require the precious structural surface shape that will not allow even thermal deformation on orbit. One design candidate to meet such severe design requirements is a smart structural system which the structural shape is actively controlled by actuators. For accurate and flexible shape control, the larger number of actuators is desired. However, as the number of actuators increases, the weight and the required power increase. This study investigates effects of the number of the actuators on the deformation error for a simple circular plate fixed at the center and deformed into the desired shape by the arranged point actuators on the plate. The actuator layout problem is formulated as the optimization problem in terms of the actuator positions and the actuator force that gives the concentrated forcein out-of-plane direction. The deformation is evaluated based on Kirchhoff-Love plate theory. Through the optimization results for some optimum actuator layout designs, efficient actuator layout design strategy is discussed. Then, the optimum design obtained through the FEM model using shell elements is investigated for the modeling verification.

1 INTRODUCTION

Space antennas for space exploration missions require a large aperture areas and high surface shape accuracy as well as light weightness. Generally, the required RMS (root mean square) error of the surface shape is said to about 1/10 $\sim$ 1/20 of the wavelength of the observation electromagnetic wave. The observation frequency about the extremely high-frequency (EHF) band (30-300GHz) will not allow even thermal deformation on orbit.

One of design candidates to meet the severe design requirement is a smart structure system which can adjust the surface shape by the implemented actuators on orbit. Recently, several studies have developed the smart space reflectors. For example, Fang et al. developed an engineering model of a membrane antenna of 2.4m diameter with adaptive surface control system [1]. The engineering model equips 168 polyvinylidene fluoride (PVDF) actuators to control the surface shape. Since an independent actuator control is impractical for the control system with such many actuators, the actuators are controlled with several groups that are arranged by a group optimization method [2]. Bradford et al. developed the active composite reflector panel with macro fiber composite (MFC) actuators to control the wavefront errors in

* kogiso@aero.osakafu-u.ac.jp

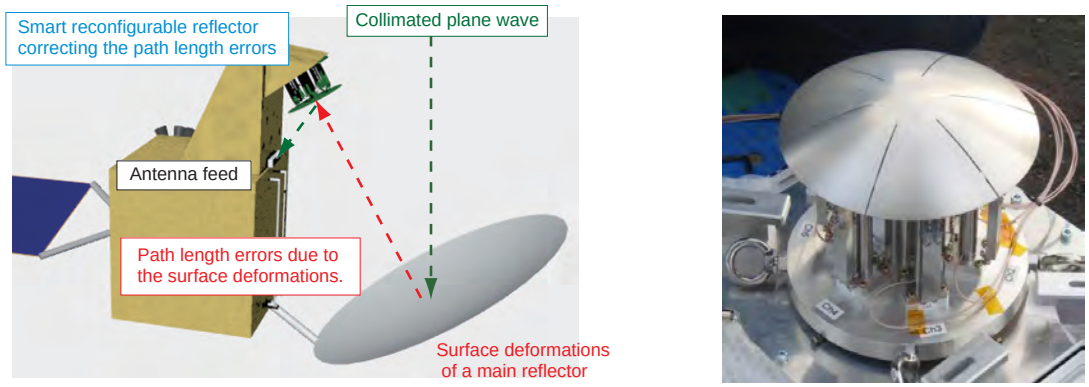

(a) High-accuracy antenna system (b) Prototype of smart reconfigurable reflector

Figure 1. High-accuracy antenna system with a smart reconfigurable reflector.

the reflector [3]. The system uses 37 actuators in each hexagonal panel with an isogrid array. Datashvili et al. developed laboratory models of reconfigurable reflectors that employed a carbon fiber-reinforced silicon (CFRS) surface with 91 actuators to control the surface shapes [4].

Since such systems with many actuators require more electric power and more complicated control strategy, and hence, reduce the reliability. Tanaka et al., one of the authors, has proposed the different space antenna system that the secondary mirror has the actuators as illustrated in Fig. 1(a) [5]. The smart secondary mirror will adjust the signal error caused by the surface error of a main reflector. As the secondary mirror is sufficient small, the required power of the actuators can be significantly reduced as well as weight.

In order to validate the strategy, the prototype of 200mm diameter secondary mirror with six Piezo actuators as shown in Fig. 1(b) has developed to demonstrate the efficiency through several measurement experiments [5]. However, the number of the actuator and the actuator layout were not optimally determined yet. In addition, the six thin slits introduced to reduce the deformation errors should have been avoided to yields some ill effects such as stress concentration.

Final objective of this study is to reduce the required number of actuators that satisfy the deformation error criteria and to obtain the optimum actuator layout with the smart reflector. As the first step, effects of the number of the actuators that give the out-of-plane concentrated force to the structure on the shape accuracy are investigated for the basic structural element through the optimization methods. In previous study, we investigated the required number of the actuators and the optimum layout for the simple cantilever beam deformed to the ideal deformation shape [6, 7]. In the study, it was found that the two actuators are sufficient to deform into the parabola by arranging the both actuators at the free edge and applying the same magnitude force to the both actuators in the opposite bending direction. That is reasonable for the cantilever problem, because the resultant actuator force is equivalent to the bending moment at the edge.

This study investigate the effects to the circular plate fixed at the center. The optimization problem is defined as minimization of the RMS error between the ideal shape and deformed shape in terms of the actuator position and the actuator force. At first, the axial symmetry condition is considered, that is equivalent to the infinite number of the actuators arranged in the circumferential direction. Then, consider the finite number of the actuator arranged at regular intervals in the circumferential direction and the effect of the number of the actuators is investigated on the RMS error.

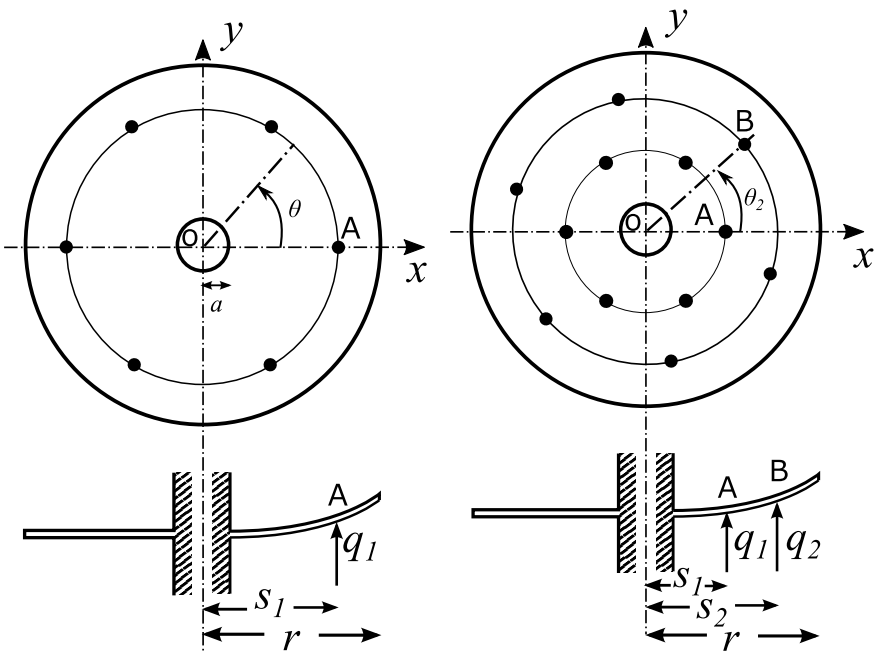

(a) Single type (b) Double type

Figure 2. Circular plate fixed at the center and actuators arranged on concentric circle

As a next step, the strategy is adopted to the FEM model using linear shell element to validate the optimization results between the theoretical model and the numerical model. In the FEM model, the actuators are located at the node that are treated as discrete design variables. On the other hand, the actuator force is modeled as a continuous design variable. For the mixed design variable problem, the evolutionary optimization method (Covariance Matrix Adaptation Evolution Strategy: CMA-ES) [8] is adopted.

Through comparison of the results between the two approaches, efficient actuator layout design is discussed. In addition, numerical result of the nonlinear FEM analysis is compared with that of the linear FEM analysis.

2 PROBLEM FORMULATION FOR BASIC PLATE THEORY

A circular plate with radius r is assumed to be fixed at the small center circle of radius a and free at the edge. Then, n actuators are allocated at n equally divided points on the concentric circle of the radius s_1 and applied the out-of-plane load q_1 as the concentrated load as shown in Fig. 2 (a). The bending deformation is evaluated based on Kirchhoff-Love plate theory [9]. For the optimum actuator layout design, the actuator position s_1 and the applied load q_1 are treated as design variables.

We will discuss the design problem with double circles illustrated in Fig. 2 (b) later. The bending deformation for such actuator allocations can be obtained by superposition of the two single type deformations under the linear deformation assumption. Though the following explanation is limited based on the single type case, it is easily extended to the double type problem.

The desired deformation shape w_I by actuators is set as a paraboloid shape as follows:

$$w_I(s,\theta) = a_I s^2 \qquad (0 \le s \le r, \quad 0 \le \theta < 2\pi) \tag{1}$$

where (s, θ) indicate the polar coordinates. a_I is a coefficient, where the maximum deformation is determined from the design requirement. In this study, it is set as 0.01 times of the plate radius as the small deformation.

2.1 Kirchhoff-Love Plate Theory

When the deformation is small, the plate deformation w by the actuator force is obtained based on Kirchhoff-Love plate theory as follows [9]:

$$w(s_1, q_1; s, \theta) = R_0(s) + \sum_{m=1}^{\infty} R_m(s)\cos(m\theta), \qquad (a \le s \le r, \quad 0 \le \theta < 2\pi) \tag{2}$$

The series terms $R_i(s), (i = 0, \cdots, m)$ are defined as follows.

$$R_0(s) = A_0 + B_0 s^2 + C_0 \log s + D_0 s^2 \log s \tag{3}$$

$$R_1(s) = A_1 s + B_1 s^3 + C_1 s^{-1} + D_1 s \log s \tag{4}$$

$$R_m(s) = A_m s^m + B_m s^{-m} + C_m s^{m+2} + D_m s^{-m+2}, \qquad (m = 2, \cdots, \infty) \tag{5}$$

where A_i, B_i, C_i, and D_i $(i = 0, \cdots, \infty)$ are determined from the boundary conditions [9].

Obviously, as the number of actuators increases, the deformation can approach the desired deformation shape. When the number of the actuators increase to infinity, the actuator load is modeled as the distributed load along the concentric circle of radius s_1. In such a case, the deformation w can be obtained through an axial symmetry model as follows [9]:

$$w_{in}(s_1, q_1; s, \theta) = \frac{q_1 s^2}{8\pi D}(\log \frac{s}{s_1} - 1) - \frac{c_1 s^2}{4} - c_2 \log \frac{s}{s_1} + c_3, \quad (a \le s \le s_1 \le r, 0 \le \theta < 2\pi)$$

$$w_{out}(s_1, q_1; s, \theta) = -\frac{c_4 s^2}{4} - c_5 \log \frac{s}{r} + c_6, \qquad (a \le s_1 \le s \le r, 0 \le \theta < 2\pi) \tag{6}$$

where w_{in} is the deformation inside of the actuator position s_1, w_{out} is that outside of the actuator position and q_1 is the total applied load. The coefficient c_1 to c_6 are determined from the boundary conditions.

2.2 Finite Element Method Model

The finite element model using linear shell elements as shown in Fig. 3 is introduced to validate the actuator layout optimization. Because the numerical model will be required for development of the actual smart reflector. The FEM model consists of 3072 elements, where the plate is equally divided into 96 pieces in the angular direction and unequally into 32 pieces in the radius direction to set the element aspect ratio properly. In this study, a semi-commercial code FEAP (Finite Element Analysis Program) [10] is adopted in this study. As the actuator can be allocated on the node, the optimization problem will be formulated as mixed design variable problem, where the actuator force is set as a continuous design variable.

2.3 Optimum Design Problem

In this study, the optimum actuator layout design problem is formulated to minimize the RMS error between the desired shape and the deformed shape in terms of the actuator position s_1 and the actuator

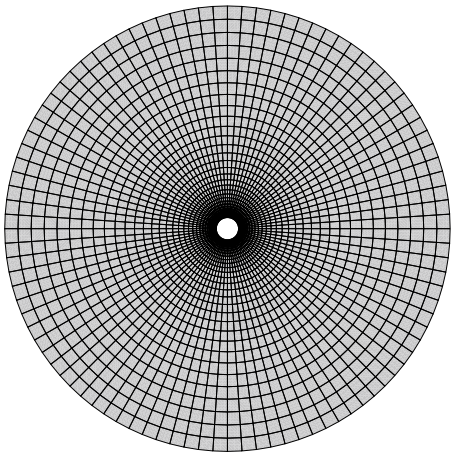

Figure 3. Finite element model of the circular plate

force q_1. The objective function is defined as the normalized RMS error as follows:

$$\text{minimize :} \qquad f_D(s_1, q_1) = \frac{f_{rms}(s_1, q_1)}{f_I} \tag{7}$$

$$\text{where :} \qquad f_{rms}(s_1, q_1) = \left(\frac{1}{\pi(r^2 - a^2)} \int_0^{2\pi} \int_a^r (w(s_1, q_1; s, \theta) - w_I(s, \theta))^2 s \, ds \, d\theta \right)^{1/2} \tag{8}$$

$$f_I = \left(\frac{1}{\pi(r^2 - a^2)} \int_0^{2\pi} \int_a^r w_I(s, \theta)^2 s \, ds \, d\theta \right)^{1/2} \tag{9}$$

where f_{rms} is the RMS error between the desired and the deformed shapes, that we would like to minimize. f_I in Eq. (9) is the normalized factor that the RMS error between the desired and the undeformed shapes. Therefore, the objective function value approaches zero as the deformation approaches the desired shape. On the other hand, the value is one for the undeformed plate.

In addition, following constraint is imposed such that the actuator should be located on the plate:

$$a \leq s_1 \leq r \tag{10}$$

For the FEM model, the RMS error is evaluated by transforming the integral to the summation with respect to the node as follows:

$$f_{rms}(s_1, q_1) = \left(\frac{1}{\sum_{k=1}^{N_n} u_i} \sum_{k=1}^{N_n} u_i (w_k - w_I)^2 \right)^{1/2} \tag{11}$$

where N_n indicates the number of the nodes and w_k corresponds to the out-of-plane deformation of the kth node. The area around the node u_i depends on the radial position as shown in Fig. 4. That is defined

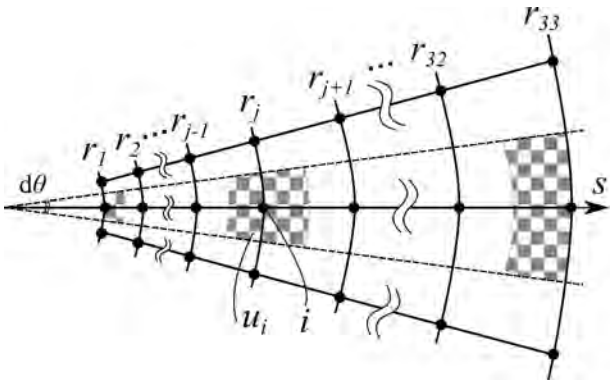

Figure 4. Area u_i around the node.

Table 1 Plate and load parameters

Plate size		Desired deformation	Plate stiffness			Actuator load	
a	r	a_I	D	ν	κ	q	p^*
0.05	1	0.01	1	0.3	$\frac{5}{6}$	$\frac{p}{p^*}$	0.03165

as follows:

$$u_1 = \left(\frac{r_2 - r_1}{2}\right)\left(\frac{3r_1 + r_2}{4}\right)\mathrm{d}\theta \tag{12}$$

$$u_i = \left(\frac{r_{i+1} - r_{i-1}}{2}\right)\left(\frac{r_{i-1} + 2r_i + r_{i+1}}{4}\right)\mathrm{d}\theta \qquad (i = 2, \ldots, 32) \tag{13}$$

$$u_{33} = \left(\frac{r_{33} - r_{32}}{2}\right)\left(\frac{3r_{32} + r_{33}}{4}\right)\mathrm{d}\theta \tag{14}$$

where r_i is the radial position of the node as shown in Fig. 4.

3 NUMERICAL INVESTIGATION AND DISCUSSION

The circular plate and the applied load are modeled as dimensionless form. The radius of the plate is set as $r = 1$ and the hole is set as $a = 0.05$. As the maximum direction of the desired shape is set as 0.01 times of the plate radius, the coefficient in Eq. (1) is set as $a_I = 0.01$. The plate bending stiffness is set as $D = 1$, the Poisson's ratio is set as 0.3 and the shear correction factor is set as $\kappa = 5/6$. The applied load is also normalized by the load applied at the edge point p^* that gives the maximum deformation 0.01 as a_I. These parameter values are summarized in Table 1.

3.1 Actuator Layout for Basic Plate Model

3.1.1 Actuator Layout on Single Concentric Circle

Consider the case that the actuators are allocated equally divided position on the single concentric circle as shown in Fig. 2(a).

Table 2 Optimal layout for actuator allocation on single concentric circle

Number of Actuators	2	3	4	5	6	8	10	12	∞
Arranged radius s_1	0.26	0.81	1.0	1.0	1.0	1.0	1.0	1.0	1.0
Normalized load q_1	2.0	2.3	1.5	1.2	0.98	0.74	0.59	0.49	0.93
Normalized RMS error	0.499	0.184	0.114	0.101	0.0985	0.0978	0.0976	0.0976	0.0971

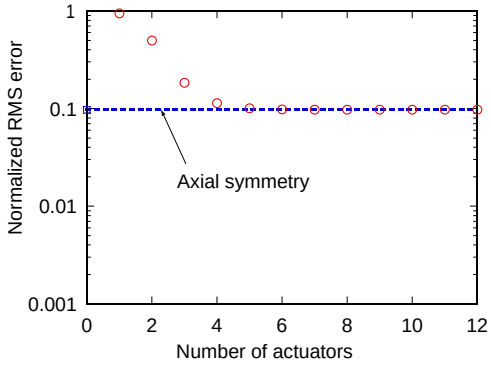

Figure 5. Optimum RMS error for actuator layout in single concentric circle

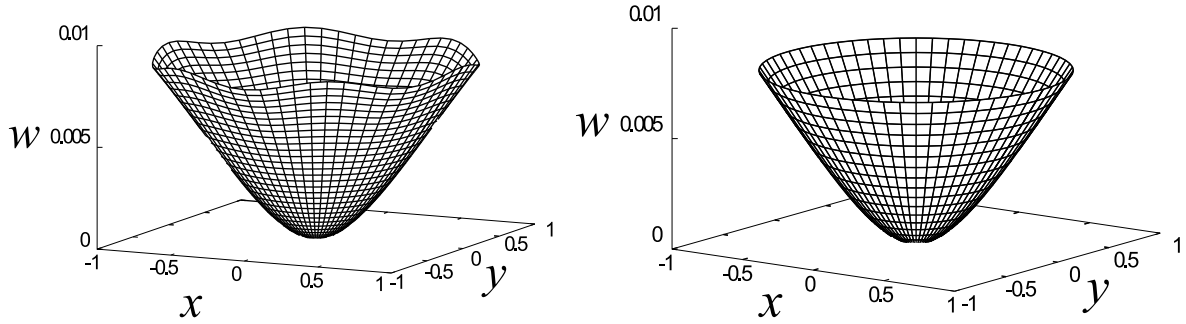

(a) $n = 6$ (b) $n = \infty$ (axial symmetry)

Figure 6. Deformation shape in optimal design in case of single concentric circle

For the deformation evaluation, the series terms in Eq. (2) is set as $m = 15$, because higher terms have found to be negligible. For the integration for evaluating the RMS error in Eqs. (8) and (9), the Gauss-Legendre integration is adopted, where the number of evaluation points is set to 20 in the radius direction and 15 in the angular direction after several preliminary calculations.

The optimization is performed by sequential quadratic method (SQP). The optimal actuator layout designs for several numbers of actuators are compared in Table 2 and Fig. 5, where $n = \infty$ corresponds to the case for the equally distributed load on the circle that is modeled as axial symmetry. As the number of the actuator increases, the actuator position converges to the edge and the RMS error decreases to converge to 0.097. For $n = 6$, the value is almost identical to that for $n = \infty$.

The deformation shapes for $n = 6$ and $n = \infty$ are illustrated in Fig. 6. The deformation for $n = 6$ is found some bumps corresponding to the actuator locations, that is different from the deformation for $n = \infty$. However, the RMS errors of both cases are almost identical with relatively large values. This

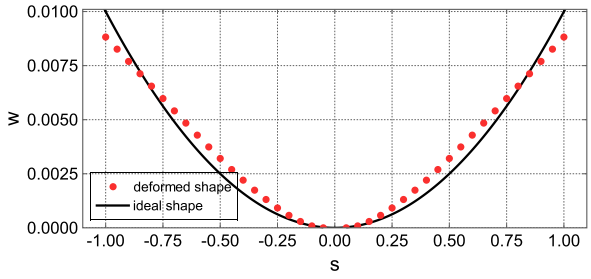

Figure 7. Cross-sectional view of deformation shape for $n = \infty$ optimum design in case of single concentric circles

Table 3 Optimal layout for actuator allocation on double concentric circles

Number of actuators	4	6	8	12	∞
Arranged radius s_1	0.590	0.788	0.860	0.924	0.874
Arranged radius s_2	0.733	0.877	0.926	0.969	0.996
Normalized load q_1	-9.09	-8.98	-8.97	-9.00	-8.97
Normalized load q_2	8.89	9.02	9.03	9.04	9.06
Shift angle θ_2	0.0	0.0	0.0	0.0	0.0
Normalized RMS error	0.883	0.0292	0.0145	0.00681	0.00398

is because the deformation curvature is opposite to the desired shape as shown in Fig. 7. That is, the actuator allocation on the single concentric circle is not sufficient to deform into the desired shape.

3.1.2 Actuator Layout on Double Concentric Circles

As the actuator allocation on the single concentric circle is not sufficient to deform into the desired shape, consider the next case that the actuators are allocated on the double concentric circles as shown in Fig. 2(b).

In this problem, the same numbers of actuators are allocated in both concentric circles with equally divided position. The actuator radial position s_i and the applied load q_i, $(i = 1, 2)$ are treated as design variables. Additionally, as the actuators on the outer circle can be shifted in the angular direction to those on the inner circle, the shift angle θ_2 are also treated as design variable. That is, the total number of design variables is five. The deformation shape is evaluated as superposition of the deformations due to the inner and the outer actuators. Each deformation is evaluated by Eq. (6).

In the optimization, the two constraints are introduced to avoid switching to the inner and the outer circles and to limit the shifting angle as follows:

$$a \leq s_1 \leq s_2 \leq r \tag{15}$$

$$0 \leq \theta_2 \leq \frac{2\pi}{n} \tag{16}$$

As in the previous studies [6, 7], this problem have many local optima in terms of the applied load. First of all, the optimal actuator layout designs for several numbers of actuators are compared in Table 3 and Fig. 8, where $n = \infty$ corresponds to the case for the equally distributed load on the circle. The

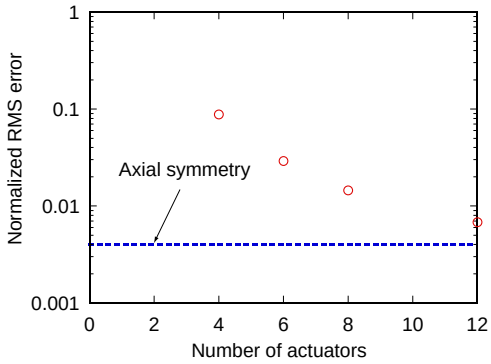

Figure 8. Optimum RMS error for actuator layout in double concentric circle

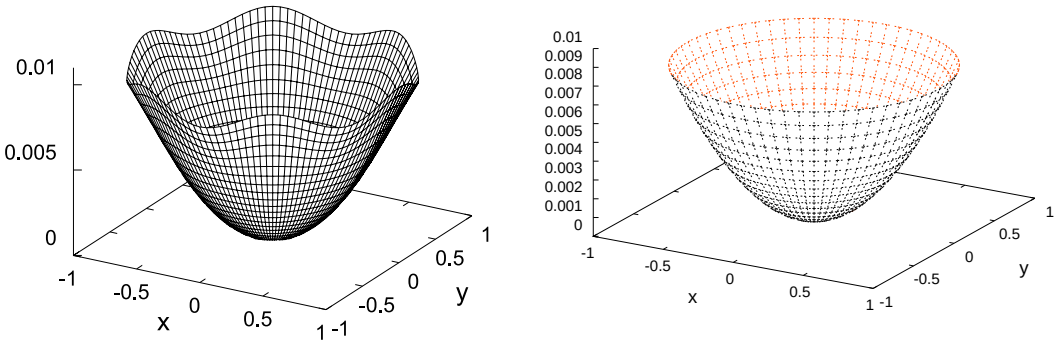

(a) $n = 6$ (b) $n = \infty$

Figure 9. Deformation shape in optimal design in case of double concentric circles

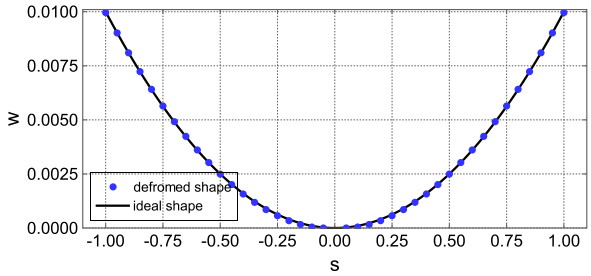

Figure 10. Cross-sectional view of deformation shape for $n = \infty$ optimum design in case of double concentric circles

two actuator positions converge to around $s_1 = 0.9$ and $s_2 = 1.0$, the applied load of the inner circle converges to -9.0 and that of the outer circle converges to 9.0. That is, for the optimum design, the actuators will apply the couple of force to the plate. As the single circle design shown in Fig. 7 has the opposite bending curvature, the design with double circles changes the bending curvature by pulling down the inner actuator.

Table 4 Local optima in Optimization results with concentrated loads

(a) $n = 6$

Position		Applied Load		Shift	Normalized
s_1	s_2	q_1	q_2	θ_2	RMS Error
0.706	0.952	-3.33	3.34	0.0	0.0297
0.749	0.913	-4.94	4.97	0.0	0.0293
0.775	0.890	-6.98	7.02	0.0	0.0292
0.788	0.877	-8.98	9.02	0.0	0.0292

(b) $n = \infty$

Position		Applied Load		Normalized
s_1	s_2	q_1	q_2	RMS Error
0.763	1.00	-4.32	4.40	0.00506
0.824	1.00	-6.02	6.11	0.00415
0.845	1.00	-6.93	7.02	0.00403
0.874	0.996	-8.97	9.06	0.00398

Table 5 Optimization results of $n = 6$ with linear FEM model

Position		Applied Load		Shift	Normalized
s_1	s_2	q_1	q_2	θ_2	RMS Error
0.709	0.940	-3.56	3.57	0.0	0.0325

The RMS error is converged to 0.00398. It means that difference from the desired shape is about 0.4% of the difference between the desired shape and the initial shape. As shown in Fig. 10, the deformation shape is almost identical to the desired shape. However, the convergence is not so good in terms of the number of actuators.

For example, the RMS error for $n = 6$ is about 10 times worse than that for $n = \infty$, though the RMS error value itself is small enough. This is because the effect of the deformation bump along the angular direction is no longer negligible.

As described above, this problem has many local optima as listed in Table 4. All local design has similar tendency that the two loads have opposite directions and the almost same magnitude. For the actual design problem, the load magnitude constraint should be considered.

In addition, the shifting angle θ_2 converged to zero for all cases. It means that the inner and the outer actuators should arrange on the same radius vector.

3.2 Finite Element Method for Double Concentrated Circles

The optimization result using FEM model shown in Fig. 3 is compared with the theoretical model with double concentrated circles. The parameters are set as the same values as listed in Table 1. As the bending stiffness D cannot set directly, Young's modulus E and the thickness h are set as 10.92×10^6 and 0.01, respectively, to $D = 1$.

As the actuators are put on node as discrete design variables, the CMA-ES (Covariance Matrix Adaptation Evolution Strategy) [8] is adopted as optimizer. The optimization result for $n = 6$ is listed in Table 5. This result is almost identical to that of the plated model listed in Table 4. The RMS error is about 10% worse than that of the plate model. This is because the actuator position is limited as nodal point.

The deformation of the optimum design cannot be avoided the bumps as illustrated in Fig. 11. As shown in the previous results, such bumps around the edges cannot be avoided by the finite number of actuators. As the bump deformation is limited to the edge, it will be a good strategy that the actuator is arranged outside of the reflector to resolve the problem [11]. In addition, the optimization of the reflector itself such as thickness distribution is another strategy.

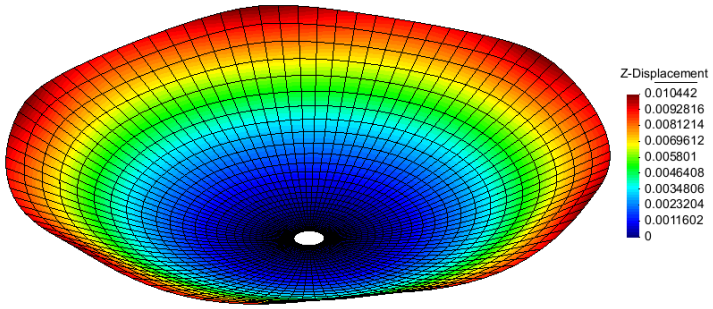

Figure 11. Deformation of the optimum actuator layout for $n = 6$

4 CONCLUSION

In this study, we consider the optimal actuator layout design that gives the out-of-plane deformation to the circular plate as the basic study of the high-precision smart structure. The optimization problem is defined as minimization of the RMS error between the desired shape and the deformed shape in terms of the actuator positions and the actuator forces in out-of-plane direction. The deformation is evaluated based on Kirchhoff-Love plate theory. Then, the optimum design for the FEM model using shell elements required for the actual design problem is investigated for verification.

Through numerical examples, the following conclusions are remarked.

- Considering the two types of the arrangements, it is found that the actuator arrangement on the double concentric circle is useful solution. However, for the limited number of actuators, the deformation with bumps around the edges cannot be avoided. Therefore, other strategy including the structural optimization or the actuator arrangement outside of the reflector should be considered in the future.
- The optimum design using FEM is found to be almost identical to that using the plate bending theory. This kind of structural modeling using FEM can be adopted for the future work to develop the smart reconfigurable mirror system.
- In FEM, the actuator position is limited on the nodal position and is treated as a discrete design variable. Therefore, the CMA-ES method is adopted as optimizer. As the evolutionary method is time consuming in comparison with mathematical programming method, more efficient optimization method or the surrogate modeling should be considered in the future.

ACKNOWLEDGEMENTS

This work is partially supported by JSPS KAKENHI Grant Number 26249131. The authors would like to express our gratitude to Prof. Iwasa, Tottori University for his valuable advice for appropriate FEAP modeling and to Mr. Taku Hagegawa, Osaka Prefecuture University for his valuable advice for the optimization using the CMA-ES algorithm.

REFERENCES

1. Fang, H., Quijano, U., Bach, V., Hill, J., and Wang, K. W. "Experimental Study of a Membrane Antenna Surface Adaptive Control System", *52nd AIAA/ASME/ASCE/AHS/ASC Structures, Structural Dynamics and Materials Conference*, 2011, AIAA 2011-1828, pp. 1-10.
2. Hill, J. R., Wang, K. W., Fang, H. and Quijano, U., "Actuator Grouping Optimization on Flexible Space Reflectors", *SPIE Proceeding*, Vol. 7977, Active and Passive Smart Structures and Integrated Systems, 2011, pp. 1-12, doi: 10.1117/12.880086.
3. Bradford, S. C., Agnes, G. S., Bach, V. M. and Wilkie, W. K., "An Active Composite Reflector System for Correcting Thermal Deformations", *52nd AIAA/ASME/ASCE/AHS/ASC Structures, Structural Dynamics and Materials Conference*, 2011, AIAA 2011-1826, pp. 1-8.
4. Datashvili, L., Baier, H., Wei, B., Hoffman, J., Wehrle, E., Schreider, L., Mangenot, C., Santiago-Prowald, J., Scolamiero, L. and Angevain J.-C., "Mechanical investigations of in-space-reconfigurable reflecting surfaces". *32nd ESA Antenna Workshop on Antennas for Space Applications*, 2010, pp. 1-8.
5. Tanaka, H., Sakamoto, H., Inagaki, A., Ishimura, K., Doi, A., Kono, Y., Oyama, T., Watanabe, K., Oikawa, Y. and Kuratomi, T., "Development of a Smart Reconfigurable Reflector Prototype for an Extremely High-Frequency Antenna", *Journal of Intelligent Material Systems and Structures*, 2015, pp. 1-10, doi:10.1177/1045389X15580660.
6. Kogiso, N., Naka, T., Ikeda, T. and Miyazaki, Y., "Basic Study Towards the Optimal Actuator Layout Design of High-Precision Smart Structure", *56th JSASS/JSME Structures Conference*, 2014, 1A12 (*in Japanese*)
7. Naka, T., Toyoda, M., Kogiso, N. and Ikeda, T., "Basic Study on Actuator Layout Design of High-Precision Smart Structure Using Robust Multiobjective Optimization", *58th Space Science and Technology Conference*, 2014, 3B04 (*in Japanese*)
8. Hansen, N, "The CMA Evolution Strategy: A Comparing Review", *Towards a New Evolutionary Computation*, Springer, 2006, pp. 75-102,
9. Timoshenko, S. P., *Theory of Plates and Shells*, McGraw-Hill, 1959, pp. 51-60, pp. 282-293.
10. Taylor, R. L., *FEAP – A Finite Element Analysis Program User Manual*, Ver. 8.3, http://www.ce.berkeley.edu/projects/feap/ (access on Oct., 2015)
11. Laslandes, M., Hugot, E., Ferrari, M., Hourtoule, C., Singer, C., Devilliers, C., Lopez, C., and Chazallet, F., "Mirror Actively Deformed and Regulated for Applications in Space: Design and Performance", *Optical Engineering*, Vol. 52, No. 9, 091803, 2013, pp. 1-12.